Preprint typeset using LaTeX style emulateapj v. 04/03/99

THE DETECTION OF OUTFLOWS IN THE IR-QUIET MOLECULAR CORE NGC 6334 I(NORTH)[a]

[a]BASED ON OBSERVATIONS CONDUCTED AT THE EUROPEAN SOUTHERN OBSERVATORY, LA SILLA, CHILE

S. T. Megeath

Harvard–Smithsonian Center for Astrophysics, 60 Garden St., Cambridge, MA 02138

A. R. Tieftrunk

Kölner Observatorium für Submm–Astronomie, 1. Physikalisches Institut der Universität zu Köln, Züplicher Str. 77, D-50937 Köln, Germany and ESO/La Silla, Casilla 19001, Santiago 19, Chile

ABSTRACT

We find strong evidence for outflows originating in the dense molecular core NGC 6334 I(North): a 1000 $M_\odot$ molecular core distinguished by its lack of H II regions and mid–IR emission. New observations were obtained of the SiO ($2 \rightarrow 1$) and ($5 \rightarrow 4$) lines with the SEST 15–m telescope and the H_2 ($\nu = 1 \rightarrow 0$) S(1) line with the ESO 2.2–m telescope. The line profiles of the SiO transitions show broad wings extending from -50 to 40 km s^{-1}, and spatial maps of the line wing emission exhibit a bipolar morphology with the peaks of the red and blue wing separated by $30''$. The estimated mass loss rate of the outflow is comparable to those for young intermediate to high–mass stars. The near–IR images show eight knots of H_2 emission. Five of the knots form a linear chain which is displaced from the axis of the SiO outflow; these knots may trace shock excited gas along the path of a second, highly collimated outflow. We propose that I(N) is a rare example of a molecular core in an early stage of cluster formation.

Subject headings: ISM:individual (NGC 6334) – ISM:jets and outflows – ISM:molecules – stars:formation

1. INTRODUCTION

At a distance of 1.7 Kpc (Neckel 1978), the NGC 6334 molecular cloud is an 11 pc long filament containing a remarkable chain of five luminous star–forming regions (McBreen et al. 1979). The youngest of these star–forming regions is thought to be the northernmost of the chain, designated NGC 6334 I in the McBreen et al. nomenclature. Evidence for the youth of this region is found in the sheer concentration of phenomena thought to accompany the earliest stages of star formation: an array of OH, H_2O, CH_3OH and NH_3(3,3) masers (Gaume & Mutel 1987; Forster & Caswell 1989; Menten & Batrla 1989; Kraemer & Jackson 1995), luminous mid–IR sources (Harvey & Gately 1983; Kraemer et al. 1999), an ultracompact H II region (DePree et al. 1995), a bipolar outflow (Bachiller & Cernicharo 1990; Davis & Eisloeffel 1995; Persi et al. 1996), and a cluster of stars detected at 1-2 μm (Tapia, Persi & Roth 1996).

The young stars of NGC 6334 I are embedded in a massive dense molecular core which has been mapped in a number of spectral lines and the submillimeter continuum. Interestingly, these same maps show that NGC 6334 I is part of a twin core system: only $2'$ north (1 pc at 1.7 kpc) of NGC 6334 I, a second dense core of roughly equal size is apparent. This second core, designated NGC 6334 I(North) [hereafter: I(N)] by Gezari (1982), has perhaps the strongest NH_3 lines observed in the sky, yielding a gas temperature of 30 K and a volume density in excess of 10^6 cm^{-3} (Forster et al. 1987; Kuiper et al. 1995). Estimates of the total mass of the cloud range from 1000 to 3000 $M_\odot$(Gezari 1982; Kuiper et al. 1995). However, in distinct contrast to source I, NGC 6334 I(N) shows no detectable H II regions, mid–IR emission, or clusters of 2 μm sources (Loughran et al. 1986; Ellingsen, Norris & McCulloch 1996; Tapia, Persi & Roth 1996).

Radio observations have detected an H_2O maser, a cluster of Class I CH_3OH masers, and a Class II CH_3OH maser toward I(N) (Moran & Rodriguez 1980; Kogan & Slysh 1998; Walsh et al. 1998). The enigmatic presence of masers without associated infrared emission or H II regions has lead to the conclusions that I(N) is a pre–stellar core about to undergo star formation (Kuiper et al. 1995) or that I(N) contains a protostar in a pure accretion phase (Moran & Rodriguez 1980). In this letter, however, we present strong evidence for outflows originating in I(N), indicating that the I(N) core already contains at least one protostar capable of driving a powerful outflow.

2. OBSERVATIONS AND DATA REDUCTION

The near–IR data were obtained over three nights in June 1998 with the IRAC2b camera on the ESO 2.2–m telescope on La Silla, Chile. The weather was photometric and the seeing was $1''$. The detector was a 256×256 pixel NICMOS3 array with a pixel scale of $0.5''$. A warm Fabry–Perot (FP) interferometer with a spectral resolution of $\lambda/\delta\lambda \sim 1000$ was used with narrow band filters acting as order sorters. Toward 16 on–source and reference positions, we obtained 3 minute integrations at ten wavelengths, including three wavelengths bracketing the H_2 ($\nu = 1 \rightarrow 0$) S(1) line, three bracketing the Br-γ line, and four wavelengths selected to measure the continuum contribution. Calibration standards were imaged at each of the FP settings. To avoid internal reflections from the FP, dome flat fields were obtained for each narrow band filter with the FP out of the optical path. The data were

reduced with a custom program written in the IDL environment.

The millimeter–wave observations were carried out in May and June 1998 using the 15–m Swedish-ESO Submillimeter Telescope (SEST). The observations were made using SIS receivers with $T_{\rm sys}$ of 100-200 K and 1440 channel acousto–optical spectrometers. The SiO $(2 \rightarrow 1)$ and $(5 \rightarrow 4)$ lines were mapped simultaneously using the dual beam–switching mode with a beam throw of $12'$ in azimuth. The ^{13}CO $(2 \rightarrow 1)$ line was subsequently mapped in position switching mode with a reference position offset by $(\Delta\alpha, \Delta\delta) = (-20', 20')$. In September 1999, ^{12}CO $(2 \rightarrow 1)$ spectra were obtained toward three positions; position switching was used with an offset of $(\Delta\alpha, \Delta\delta) = (30', 0')$. The FWHP beamwidths are $58''$ for SiO $(2 \rightarrow 1)$ and $23''$ for SiO $(5 \rightarrow 4)$, ^{13}CO $(2 \rightarrow 1)$ and ^{12}CO $(2 \rightarrow 1)$. The velocity widths per channel (typical RMS noises per channel) are 2.39 (0.03), 0.97 (0.04), 0.95 (0.10) and 0.95 km s^{-1} (0.12 K) for the SiO $(2 \rightarrow 1)$, SiO $(5 \rightarrow 4)$, ^{13}CO $(2 \rightarrow 1)$, and ^{12}CO $(2 \rightarrow 1)$ lines, respectively. Using the CLASS package, 1st and 3rd order baselines were subtracted from the SiO and CO data, respectively. The temperatures were calibrated using the chopper–wheel method and placed on a main–beam brightness temperature scale using the beam efficiences given in the SEST Handbook ver2.1 (1998). The pointing corrections never exceeded $5''$.

3. ANALYSIS

We mapped the SiO $(5 \rightarrow 4)$ and $(2 \rightarrow 1)$ lines in a 5×5 grid with $20''$ spacings centered on the I(N) core. SiO line emission is detected in both transitions at all 25 map positions. Broad wings are detected in both the $(2 \rightarrow 1)$ and $(5 \rightarrow 4)$ spectra at velocities ranging from $V_{lsr} = -50$ km s^{-1} to 40 km s^{-1}. In Fig. 1, we display SiO $(2 \rightarrow 1)$ and $(5 \rightarrow 4)$ spectra toward the positions showing the strongest blue and red wing emission.

The velocity integrated SiO $(5 \rightarrow 4)$ emission of the red wing, blue wing, and line core are plotted in Fig 2. The wings are integrated over the velocity range in which wing emission is apparent in *both* the SiO $(5 \rightarrow 4)$ and $(2 \rightarrow 1)$ lines and is clearly separable from the line core. Higher spectral resolution SiO $(2 \rightarrow 1)$ and $(3 \rightarrow 2)$ data show the wings extending into the -15 to 7.5 km s^{-1} velocity interval of the plotted line core emission (Tieftrunk & Megeath 1999); however, this low velocity wing component cannot be isolated in the low spectral resolution data presented here.

The SiO line core emission is sharply peaked at a position of $\alpha_{1950} = 17^h17^m34.3^s$, $\delta_{1950} = -35°42'10''$, coincident to within $10''$ of the peaks of the dense gas tracers HC_3N $(15 \rightarrow 14)$, CS $(7 \rightarrow 6)$ and $NH_3(3,3)$ (Megeath & Sollins 1999; Kraemer & Jackson 1999) and of the peak of the 350 – 1100 μm continuum emission (Sandell 1999). The red wing peaks $10''$ to the north of the center of I(N) (as defined by the peak core emission); the stronger, more spatially extended blue wing peaks $20''$ to the southeast of the center. The spatial offset of the red and blue wings is also apparent in the position–velocity diagram (Fig. 2). The positions of the peaks are not dependent on the adopted integration intervals or the choice of contours. The detection of broad wings which peak within $20''$ of the center of I(N), and which exhibit a spatial offset between the blue and red–shifted emission peaks, is strong evidence for a bipolar outflow originating in I(N).

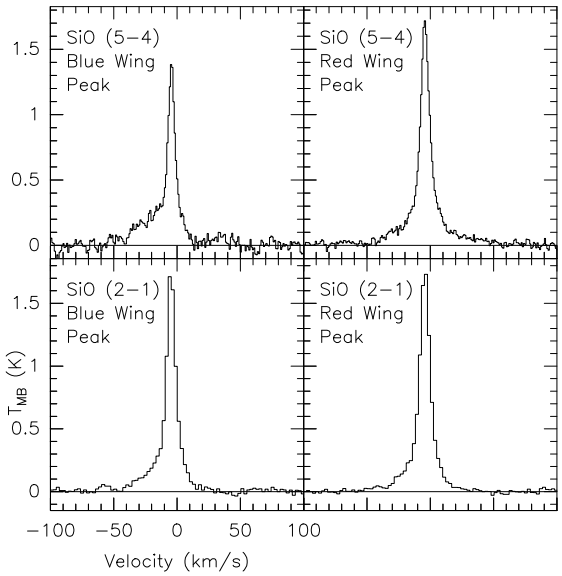

FIG. 1.— Spectra of the SiO $(2 \rightarrow 1)$ and SiO $(5 \rightarrow 4)$ emission lines toward NGC 6334 I(N). Displayed are the spectra at the peak positions of the blue and red wings.

The column density of SiO in the outflow is determined independently for each 5 km s^{-1} velocity interval from $V_{lsr} = -50$ to -15 km s^{-1} for the blue wing and from 10 to 40 km s^{-1} for the red wing. Assuming optically thin emission and convolving the SiO $(5 \rightarrow 4)$ data to the beamsize of the SiO $(2 \rightarrow 1)$ data $(58'')$, we calculate the column density in the $J = 2$ and $J = 5$ states and estimate a rotational temperature from the ratio of these column densities (Goldsmith & Langer 1999). The rotational temperatures are ~ 10 K for all of the velocity intervals. Assuming a constant rotational temperature between all of the rotational states, a total SiO column density is determined for each velocity interval. The 10 K rotational temperature is significantly less than the 30 K kinetic temperature of the core (Kuiper et al. 1995), indicating that the SiO is subthermally excited. A statistical equilibrium simulation with a large velocity gradient approximation shows that for kinetic temperatures of 30 to 100 K and volume densities of 10^6 cm^{-3} to 3×10^5 cm^{-3}, the distribution of molecules among the rotational states can be well approximated by a contant rotational temperature with a value of ~ 10 K. With these simulations, we estimate that the errors incurred by our assumption of a constant rotational temperature are less than 20%.

The derivation of the outflow properties require an in situ measurement of the abundance of SiO relative to H_2, as the SiO abundance can be enhanced by orders of magnitude in outflows (Acord, Walmsley & Churchwell 1997; Codella, Bachiller & Reipurth 1999). We use the ^{13}CO $(2 \rightarrow 1)$ spectra to determine the column density of H_2. Toward the peak position of the blue SiO line wing emission, the ^{13}CO $(2 \rightarrow 1)$ spectra shows a clear detection of the blue line wing. We limit our analysis to the velocity range of $V_{lsr} = -20$ to -15 km s^{-1}, over which the ^{13}CO $(2 \rightarrow 1)$ wing has a high signal–to–noise and shows no troughs indicative of contaminating emission in the ref-

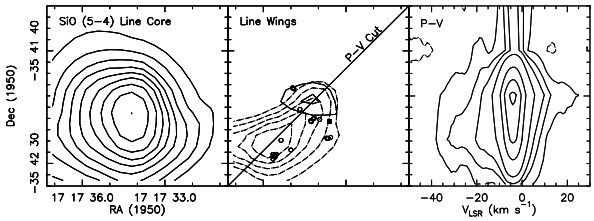

FIG. 2.— The SiO ($5 \rightarrow 4$) line emission. Left panel: the line core emission integrated over $V_{lsr} = -15$ to 7.5 km s^{-1}. The contour levels are 3.9 to 17.55 by 1.95 K km s^{-1}. Middle panel: the dashed contours show the blue–shifted line wing emission integrated over $V_{lsr} = -50$ to -15 km s^{-1} and the solid contours show the red–shifted gas integrated over $V_{lsr} = 7.5$ to 40 km s^{-1}. The contour levels are 2.5 to 4.5 by 0.5 K km s^{-1}. The open circles mark the 44 GHz Class I methanol masers (Kogan & Slysh 1998), and the filled square marks the 6 and 12 GHz Class II methanol maser (Walsh et al. 1998). Right panel: the position–velocity diagram along the the diagonal cut shown in the middle panel. The velocity resolution is smoothed to 4.9 km s^{-1}. The contour levels are -0.03, 0.07, 0.14, 0.21, 0.35 to 1.40 by 0.35 K

erence beam. The ratio of the ^{12}CO to ^{13}CO temperatures at this position and velocity range indicate that the ^{13}CO is optically thin with an optical depth of 0.1. We adopt a kinetic temperature of 30 K (Kuiper et al. 1995) and assume LTE, resulting in a ^{13}CO column density of 4.6×10^{14} cm^{-2} averaged over a 58″ FWHP beamwidth and integrated over the -20 to -15 km s^{-1} velocity interval. Assuming a ^{12}C/^{13}C ratio of 59 (Wilson & Rood 1994) and a [CO]/[H_2] abundance of 10^{-4}, the column density of H_2 is 2.7×10^{20} cm^{-2}. For the identical velocity interval and beamwidth, the SiO column density is 2.2×10^{12} cm^{-2} and the resulting relative abundance is [SiO]/[H_2] $= 8 \times 10^{-9}$. This value is similar to that derived in the outflow of the neighboring NGC 6334 I core by Bachiller & Cernicharo (1990). The estimated abundance decreases with an increase in the adopted kinetic temperature: a temperature of 100 K yields [SiO]/[H_2] $= 3 \times 10^{-9}$. A similar analysis of the SiO column density in the Gaussian–shaped line cores and a H_2 column density derived from C^{18}O measurements (Megeath & Sollins 1999), results in an SiO relative abundance of 2×10^{-10} for the low–velocity and quiescent gas in I(N), showing that the SiO abundance is enhanced in the high velocity gas.

TABLE 1

Property	Blue Wing	Red Wing
Mass	4.9 $M_\odot$	2.0 $M_\odot$
Momentum	110 $M_\odot$ km s^{-1}	46 $M_\odot$ km s^{-1}
Energy	3.0×10^{46} ergs	1.2×10^{46} ergs
Mass Loss[a]	1.0×10^{-3} $M_\odot$ yr^{-1}	0.4×10^{-3} $M_\odot$ yr^{-1}
Luminosity[ab]	51 $L_\odot$	20 $L_\odot$

[a]Adopting an age of 5000 years (see text). [b]The luminosity is the mechanical luminosity given by the energy over the age.

Adopting a SiO relative abundance of 8×10^{-9}, we estimate a total momentum and energy using the equations given in Choi, Evans & Jaffe (1993). To calculate the dynamical timescale, we take the outflow radius to be 15″ (or 0.12 pc), half the distance between the emission peaks of the line wings in Fig. 2, and divide by the mass–weighted average velocity to obtain a value of 5000 years. The derived outflow properties are listed in Table 1. These values are not corrected by an assumed inclination angle.

Independent evidence for an outflow in I(N) is shown in our continuum subtracted image of the 2.12 μm H_2 ($\nu = 1 \rightarrow 0$) S(1) emission (Fig. 3). Through a careful inspection of the images, we have identified eight knots of H_2 emission toward I(N). The brightest of the knots is the nebula detected in broad band 2.2 μm imaging by Tapia, Persi & Roth (1996). The lack of any known UV sources in I(N) capable of fluorescing H_2 molecules, the distribution of the H_2 emission in widely separated, compact knots, and the absence of continuum emission toward the H_2 knots suggests that the knots are shock–excited nebulae in one or more outflows. The knots are to the northwest of the SiO outflow, and they possibly trace the continuation of the redshifted lobe of the outflow. However, five of the knots fall in a linear chain which is displaced from the axis of the bipolar outflow detected in SiO. This geometry suggests that these five knots may trace a second, highly collimated outflow in I(N).

4. DISCUSSION

The detection of the bipolar molecular outflow is strong evidence for ongoing star formation in NGC 6334 I(N). The presence of outflows, and the implication that the core is not starless, provides an explanation for the enigmatic presence of CH_3OH and H_2O masers in the core. Indeed, the detected masers are coincident with the observed high velocity gas (Fig. 2). Since the driving source of the SiO outflow has not been directly detected, the source properties must be inferred from the properties of the outflow, with the constraint that the source luminosity must be less than the total core luminosity of 10^4 $L_\odot$ derived from submillimeter observations (Gezari 1982). Shepherd & Churchwell (1996) have found a relationship between source luminosity vs. mass loss rate for luminosities ranging from 1 to 10^5 $L_\odot$.

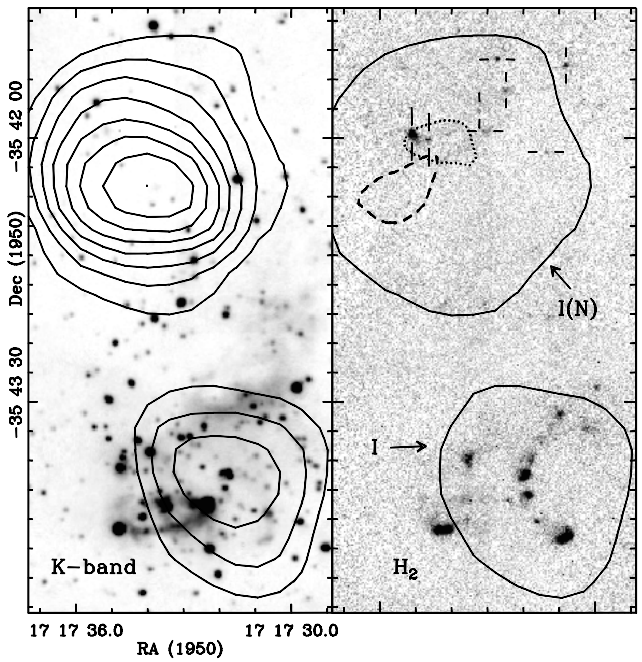

FIG. 3.— Left panel: a K–band image with contours of HC_3N ($15 \rightarrow 14$) emission overlaid; the contour levels are 5.19 to 17.3 by 1.73 K km s^{-1}(Megeath, Sollins & Wilson 1999). The NGC 6334 I region is centered on the southern HC_3N clump; the northern clump is the NGC 6334 I(N) core. A dense cluster of 2 μm sources is apparent toward I. Right panel: the continuum subtracted H_2 ($\nu = 1 \rightarrow 0$) S(1) emission. Overlayed are the contours of the blue (4.0 K km s^{-1}; dashed) and red (2.5 K km s^{-1}; dotted) SiO ($5 \rightarrow 4$) line wings and the integrated HC_3N ($15 \rightarrow 14$) emission (5.19 K km s^{-1}; solid). A complex of H_2 emission knots is visible toward I. Toward I(N), the positions of the eight H_2 emission knots are marked. The five knots tracing a possible collimated outflow are marked by the vertical lines.

The mass loss rate of the NGC 6334 I(N) outflow, 10^{-3} $M_\odot$ yr^{-1}, is characteristic of sources with luminosities of 10^3 $L_\odot$. Due to the unknown inclination of the outflow, the actual mass loss rate can be substantially different; however, it is unlikely that the resulting uncertainty in the luminosity is more than a factor of ten. Consequently, the driving source is probably a deeply embedded intermediate to high–mass (proto)star.

It is likely that I(N) is forming multiple stars. The geometry of the H_2 knots is suggestive of at least one additional outflow, driven by a second, embedded source. The detection of five faint, highly reddened ($H - K > 1.6$) near–IR point sources and three distinct submillimeter condensations within the confines of the I(N) core is further evidence for multiple sites of star formation (Tapia, Persi & Roth 1996; Sandell 1999). Additionally, the mass, density and size of the I(N) core are comparable to those of cluster–forming cores; Fig. 3 shows that the similar NGC 6334 I core contains a cluster of more than 90 stars (Tapia, Persi & Roth 1996). For these reasons, we propose that NGC 6334 I(N) is a rare example of a molecular core in the early stages of cluster formation. We predict that I(N) will evolve into a region similar to the active I core, with a pronounced cluster of 2 μm sources, H II regions and luminous mid–IR sources. A longstanding question is whether star formation in clusters progresses in a sequence, starting with the low–mass stars and ending with the formation of high–mass stars. If the NGC 6334 I(N) core is in the process of forming a cluster, then the formation of at least one intermediate to high–mass star has preceeded the *appearance* of a dense cluster of low–mass stars. This does not necessarily imply that high–mass star formation has preceeded the *formation* of most of the low–mass stars; the low–mass stars may be hidden by the high extinction in the core. These results do imply that the earliest stages of cluster formation may be identified not by bright mid–IR emission, H II regions or dense clusters of 2 μm sources, but by the presence of powerful outflows and masers detectable at radio wavelengths. Surveys for masers and outflows, particularly in regions without mid–IR sources, is a promising means for identifying molecular cores at the onset of cluster formation.

We thank S. Hüttemeister and T. Bergin for providing results from their LVG codes, P. Myers, P. Sollins and Q. Zhang for commenting on this manuscript, and K. Kraemer, J. Jackson, K. Menten, G. Sandell and P. Pratap for valuable discussions.

REFERENCES

Acord, J., Walmsley, C. M. & Churchwell, E. 1997, ApJ, 475, 693
Bachiller R. & Cernicharo, P. 1990, A&A, 239, 276
Choi, M., Evans II, N. J. & Jaffe, D. T. 1993, ApJ, 417, 624
Codella, C., Bachiller, R. & Reipurth, B. 1999, A&A, 343, 585
Davis, C. J. & Eisloeffel, J. 1995, ApJ, 300, 851
DePree, C. G., Rodriguez, L. F., Dickel, H. R. & Goss, W. M. 1995, ApJ, 447, 220
Ellingsen, S. P., Norris, R. P. & McCulloch, P.M. 1996, MNRAS 279, 101
Forster, J. R., Whiteoak, J. B., Gardner, F. F., Peters, W. L. & Kuipers, T. B. H. 1987, Proc. ASA, 7, 189
Forster, J. R. & Caswell, J. L. 1989, A&A, 213, 339
Gaume, R. A. & Mutel, R. B. 1987, ApJS, 65, 193
Gezari, D. Y. 1982, 259, L29
Goldsmith, P. F. & Langer, W. D. 1999, ApJ, 517, 209
Harvey, P. M. & Gately, I. 1983, ApJ, 269, 613
Kogan, L. & Slysh, V. 1998, ApJ, 497, 800
Kraemer, K. E. & Jackson, J. M. 1995, ApJ, 439, L9
Kraemer, K. E., Deutsch, L. K., Jackson, J. M., Hora, J. L., Fazio, G. G., Hoffmann, W. F. & Dayal, A. 1999, ApJ, 516, 817
Kraemer, K. E. & Jackson, J. M. 1999, ApJ, in press.
Kuiper, T. B. H., Peters III, W. L., Foster, J. R., Gardner F. F. & Whiteoak, J. B. 1995, ApJ, 446, 692
Loughran, L, McBreen, B., Fazio, G. G., Rengarajan, T. N., Maxson, C. W., Serio, S., Sciortino, S. & Ray, T. P. 1986, ApJ, 303, 629
McBreen, B., Fazio, G. G., Steir, M. & Wright, E. L. 1979, ApJ, 232, L183
Megeath, S. T., Sollins, P., & Wilson 1999, in prep.
Menten, K. M. & Batrla, W. 1989, ApJ, 341, 839
Moran, J. M. & Rodriguez, L. F. 1980, ApJ, 236, L159
Neckel, T. 1978, A&A, 69, 51
Persi, P., Roth, M., Tapia, M., Marenzi, A. R., Felli, M., Testi, L. & Ferrari-Toniolo, M. 1996, A&A, 307, 591
Sandell, G. 1999, A&A, in press.
Shepherd, D. S. & Churchwell, E. 1996, ApJ, 472, 225
Tapia, M., Persi, P. & Roth, M. 1996, A&A, 316, 102
Tieftrunk, A. R. & Megeath, S. T. 1999, in prep.
Walsh, A. J., Burton, M. G., Hyland, A. R., & Robinson, G. 1998, MNRAS, 301, 640
Wilson, T. L & Rood, R. T. 1994, ARA&A, 32, 192